DEUTSCHES ELEKTRONEN-SYNCHROTRON DESY

DESY SR-75/14
October 1975

Perfect Crystal Monochromators for Synchrotron X-Radiation

by

U. Bonse, G. Materlik and W. Schröder
Institut für Physik, Universität Dortmund

2 HAMBURG 52 · NOTKESTIEG 1

To be sure that your preprints are promptly included in the
HIGH ENERGY PHYSICS INDEX ,
send them to the following address (if possible by air mail) :

DESY
Bibliothek
2 Hamburg 52
Notkestieg 1
Germany

Perfect Crystal Monochromators for Synchrotron X-Radiation

by

U. Bonse, G. Materlik and W. Schröder,
Institut für Physik, Universität Dortmund, D-4600 Dortmund 50,
POB 50 0500 , Germany.

Some techniques are surveyed how to monochromatize synchrotron X-radiation and to eliminate harmonics in the most appropriate way. The theoretical estimates are compared with spectral intensity distribution measurements at DESY in Hamburg and found in good agreement.

1. Introduction

The usefulness of synchrotron radiation for investigations in the X-ray region is gradually becoming known to X-ray scientists. Applications so far reported include measurements of the diffraction by biological samples (Barrington-Leigh, Holmes & Rosenbaum, 1972; Holmes, 1974), interferometric measurements of the anomalous dispersion occuring near absorption edges (Bonse, Materlik & Schröder, 1974; Bonse & Materlik, 1974; 1975), single crystal topography of the defect structure in crystals (Tuomi, Naukkarinen, Laurila & Rabe, 1973; Tuomi, Naukkarinen & Rabe, 1974; Bart, 1975) and EXAFS-Studies (Kincaid & Eisenberger, 1975).

Synchroton radiation has, when compared to conventional X-ray sources, some outstanding properties, which we might list as follows:

(1) The continous wavelength spectrum which, depending on the maximum energy of the orbiting electrons, may well extend form 0.1 Å X-rays up to visible light,

(2) the high intensity per wavelength range $\Delta\lambda$ (spectral luminosity),

(3) the high intensity per solid angle $\Delta\Omega$ (angular luminosity) in the X-ray range where the radiation cone is relativistically compressed into a narrow region in the forward direction,

(4) the relatively small angular size of the effective source and

(5) up to 100% polarisation of the radiation emitted within the orbital plane.

In order to exploit the virtues of synchrotron radiation fully X-ray diffraction experiments have to be adapted to the special source characteristics in a suitable way. If this is done then in most cases the speed of experiments may be increased up to several orders of magnitude. Furthermore, with synchrotron ra-

diation, some new experiments and applications of X-radiation became feasable for the first time.

A major role in this context plays the mode of monochromatization. On one hand the continuous spectrum provides any X-ray wavelength which might be needed in a particular experiment, on the other it implies the necessity of monochromatization if in the course of the experiment only one certain wavelength λ with a given spread $\Delta\lambda$ is wanted at a time. In such a case, contrary to the situation with a conventional source emitting characteristic lines, the elimination of higher harmonics may become the essential problem.

As we will show below, the elimination of harmonics can very effectively be accomplished by combining for instance Bragg and Laue case diffraction. For the benefit - as we hope - of further diffraction experiments we therefore report on successful techniques of how to monochromatize synchrotron radiation. Some of the methods we have checked experimentally. All measurements were made at DESY in Hamburg.

2. Radiation characteristics of DESY in the X-ray region

In order to give some quantitative estimates of intensities etc. we start by summarizing briefly the X-radiation characteristics of DESY as calculated form the formula by Schwinger (1949). All data are based on an effective electron orbit radius

r = 31.7 m, an injection frequency of 50 Hz, a beam current of 10 mA and an intercepting slit 0.5 mm wide by 7 mm heigh at a distance of 29 m from the emission point of the electron orbit what corresponds to a vertical and horizontal divergence of $\pm$ 1.2 x 10^{-4} and $\pm$ 8.6 x 10^{-6} rad respectively. The horizontal divergence, however, actual present in a beam passing through the interception slit is considerably larger since it is enlarged due to the finite horizontal extension of the electron beam of about 10 mm. From the horizontal size we calculate the effective horizontal divergence to roughly $\Delta\theta$ = 3.5 x 10^{-4}. With this divergence a fixed crystal reflects a certain λ-range $\Delta\lambda/\lambda = \cot\theta\ \Delta\theta$. For the silicon 111 (220) reflection of radiation at λ = 1.54Å we calculate $\Delta\lambda$ = 2.1 x10^{-3} Å (1.23 * 10^{-3} Å) respectively. To come close to a realistic case we therefore calculated the number of photons for a wavelength range of $\Delta\lambda = 10^{-3}$ Å.

The results calculated under the conditions stated before are presented in Fig. 1 through Fig. 8. Fig. 1 gives the total number of photons passing the slit per second as a function of λ and for five different maximum electron energies E_{max} ranging from 4 GeV to 7.2 GeV. Fig. 2 shows the distribution of photons in the polarisation states perpendicular ($\perp$) and parallel ($\parallel$) to the orbit plane for 5 and 7.2 GeV respectively. For λ = 1.5Å and 0.75Å the variation of photon numbers in states $\perp$ and $\parallel$ with the inclination angle ψ against the orbit plane is

illustrated in Fig. 3 for 5 GeV and in Fig. 4 for 7.2 GeV respectively. $\Delta\psi = 10^{-5}$ rad corresponds to about 0.3 mm (vertical) travel within the slit system. It is seen that at the position of the slit there are practically no $\perp$ photons within $\pm$ 100 µm of the aequatorial (orbital) plane.

The data of Fig. 3 and Fig. 4 have been obtained with the assumption that the height of the electron beam is small compared to the slit height. The effective beam height was found to depend on the operational parameters of the synchrotron and to vary between roughly 1 mm and 4 mm. Therefore, in order to reflect the experimental situation properly, the profiles of Fig. 3 and Fig. 4 ought to be smeared out correspondingly. The high degree of polarization of the total radiation within the slit is nevertheless not considerably affected by the smearing procedure. Consequently, if the Bragg diffraction by the crystal monochromator also favours one polarisation state, for instance if 2θ near $\pi/2$ or if Laue case diffraction by a thick perfect crystal is employed, then, in order to secure high intensity, the plane of incidence of the diffraction must be oriented at right angles to the orbit plane.

Fig. 5 and Fig.6 show the variation of the number of photons per second with the location within the slit for λ = 1.5, 0.75 and 0.32 Å and for E_{max} = 5 GeV and 7.2 GeV respectively. The numbers

of photons in states $\perp$ and $\parallel$ have been added. Apparently in the center of the slit the intensity distribution is nearly uniform whereas near the top and the bottom there is a sharp drop off. The shorter the wavelength the smaller is the useful vertical divergence.

Fig. 7 and Fig. 8 show the calculated time dependence of photon rates whithin one accelerating cycle of the synchrotron for a variety of wavelengths and E_{max} = 5 GeV and E_{max} = 7.2 GeV respectively. It is seen that only near the end of the 10 ms cycle high X-ray photon rates are obtained. The time intervals during which the photon rates are at least 1% of their peak value range from a minimum value of about 3 ms (λ = 0.35 Å and E_{max} = 5 GeV) to a maximum of about 6 ms (λ = 3.0 Å and E_{max} = 7.2 GeV. The puls structure due to the orbital and bunch frequencies is not resolved. The pulsing characteristics of the source facilitates the use of detector gating techniques for overall background reduction ; on the other hand it might require a high time resolution of the detectors.

3. Monochromatization by a double reflection groove

As was shown some years ago (Bonse & Hart 1965) multiple Bragg reflection by a groove cut in a perfect crystal may be used as a simple means to suppress the tails of dynamical single crystal

reflection curves considerably. At the synchrotron we used a twofold Si 220 reflection groove housed in a lead shield shown in Fig. 9. With the lead housing it was possible to eliminate the undiffracted parts of the primary beam almost completely even at such high electron energies as 7.2 GeV.

In order to reduce the general background near the measuring facility we found it essential to use exactly the wanted wavelength range of the primary beam and suppress all the rest right at the exit of the beam pipe. This can be achieved by the shielded groove monochromator except for the elimination of harmonics. The wavelength to be selected can be adjusted by rotating the monochromator about an axis normal to the drawing. The geometry of the groove is such that with the 220 reflection λ can be varied between $\lambda_{min} = 1.3$ Å and $\lambda_{max} = 1.9$ Å. Neighbouring λ-ranges can be covered by a set of groove monochromators with suitable geometries, materials and reflection orders.

The diffracted radiation behind the groove monochromator was analysed with a solid state detector (SSD) combined with a multichannel analyser. The result is shown in a logarithmic scale in Fig. 10. The harmonics up to $\lambda/6$ are all present. Over the λ-regions between the harmonics the intensity is down to below 10^{-3} of the first peak. Even higher suppression can be obtained with grooves of triple, quadruple or fivefold Bragg reflection at no more than 25% loss of intensity in the peaks.

By varying the angle of incidence any other set of fundamentals and corresponding harmonics can be selected from the continum. Thus already with just this one groove a set of X-ray "lines" between 0.3 Å (shortest harmonic) and 1.9 Å (longest fundamental) is accessible.

4. Elimination of harmonics

4.1 Principal methods

Harmonics may be eliminated by making the diffracting system wavelength dependent (dispersive). With harmonics it is the task of making the system just about dispersive enough and not more in order not to waste intensity. The classical high dispersive system is the double crystal diffractometer (Ehrenberg & Mark, 1927) in the (+, +) setting (Fig. 11a) or its recent multiple reflection version discussed by Beaumont & Hart (1974) for synchrotron X-ray spectroscopy. A system which is only slightly dispersive is the double crystal diffractometer in (+, -) setting with two reflections with different Bragg plane spacings d_1 and $d_2 = d_1 + \Delta d$ where $|\Delta d| << d_1$ (Fig. 12a). DuMond diagrams (DuMond, 1937) of these cases are shown schematically in Fig. 11b and 12b. From them the dispersive range $\Delta\lambda$ of a system may be estimated. It is easily seen that $\Delta\lambda/\lambda$ is the smaller the larger the angle between the DuMond curves of the two crystals. Other dispersive multiple reflection arrangements, for instance similar to those mentioned by Kikuta & Kohra (1970) might also be considered.

For separating the harmonics from their fundamental wave $\Delta\lambda/\lambda \approx 0.8$ should be sufficient. The (+, +)-setting with $\Delta\lambda/\lambda \approx 10^{-6} \ldots 10^{-4}$ is extremely intensity wasting. The far less wasting slightly dispersive (+, -)-setting may be used as will be shown.

However there exists another method saving even more intensity in the harmonics elimination operation. The fundamental idea behind it is to employ consecutively two single crystal reflections for which the refractive index correction to the Bragg angle is different for the fundamental and for the harmonics. Thus by adjusting the relative orientation of the crystals with respect to each other either the fundamental alone or one of the harmonics may be selected.

Let $\beta_{\pm}^{(n)}$ be the orientation difference of crystals I and II for the two settings as defined in Fig. 11 a and Fig. 12 a in the particular case where the crystals have been adjusted so that the n-th harmonic is maximized:

$$\beta_{\pm}^{(n)} = \ominus_{I}^{(n)} \pm \ominus_{II}^{(n)} \qquad (1)$$

In (1) $\ominus_{I,II}^{(n)}$ is related to the Bragg angle $\ominus_{BI,II}$ calculated from Bragg's equation and the correction $\Delta\ominus_{I,II}^{(n)}$ due to refraction according to

$$\ominus_{I,II}^{(n)} = \ominus_{BI,II} + \Delta\ominus_{I,II}^{(n)} \qquad (2)$$

where (LAUE, 1960)

$$\Delta\Theta_{I,II}^{(n)} = \frac{r_e \lambda^2}{2\pi n^2} \frac{N_{I,II}}{\sin 2\Theta_{BI,II}} \left(1 - \left(\frac{\gamma_h}{\gamma_0}\right)_{I,II}\right) \qquad (3)$$

In (3) r_e is the classical radius of the electron, $N_{I,II}$ is the number of electrons per unit volume and

$$\gamma_{hI,II} := \sin\left(\varphi_{I,II} - \Theta_{BI,II}\right), \quad \gamma_{oI,II} := \sin\left(\varphi_{I,II} + \Theta_{BI,II}\right)$$

with $\varphi_{I,II}$ the angle between the surface and the net planes used in the reflection. For Laue geometry $\gamma_h/\gamma_o > 0$ and for Bragg geometry $\gamma_h/\gamma_o < 0$. Of importance is the difference

$$\Delta\beta_{\pm}^{(m,n)} := \beta_{\pm}^{(m)} - \beta_{\pm}^{(n)} \qquad (4)$$

occuring between the maximum settings of the harmonics of order n and m. Obviously only if $|\Delta\beta_{\pm}^{(m,n)}|$ is large enough compared to the reflection widths of either harmonic then separation is feasable. With equations (1) through (4) we calculate in a straightforward manner

$$\Delta\beta_{\pm}^{(m,n)} = \frac{r_e \lambda^2}{2\pi}(m^{-2} - n^{-2})\left[\frac{N_I\left(1 - \left(\frac{\gamma_h}{\gamma_o}\right)_I\right)}{\sin 2\Theta_{BI}} \pm \frac{N_{II}\left(1 - \left(\frac{\gamma_h}{\gamma_o}\right)_{II}\right)}{\sin 2\Theta_{BII}}\right] \qquad (5)$$

Note that if both crystals reflect in the symmetrical Laue case then in the (+,-)-setting $\Delta\beta_{\pm}^{(m,n)} = 0$ whatever materials and reflection orders are used.

In the following we discuss two special cases of equation (5) where the separation of the fundamental $\lambda = \lambda^{(1)}$ from all harmonics $\lambda^{(n)}$ is possible and which we also have checked experimentally.

4.2 Symmetric Si 220 - Ge 220 (+, -) Bragg case setting

With two symmetrical Bragg cases $(\gamma_h/\gamma_o)_{I,II} = -1$. Considering the separation of the n-th harmonic from the fundamental we have to set m = 1 and find from (5)

$$\Delta\beta_-^{(1,n)} = \frac{r_e \lambda^2}{\pi}\left(1 - n^{-2}\right)\left[\frac{N_I}{\sin 2\theta_{B,I}} - \frac{N_{II}}{\sin 2\theta_{B,II}}\right] \qquad (6)$$

For the first harmonic (n = 2), $\lambda = 1.54$ Å and the Si 220 - Ge 220 combination we calculate $|\Delta\beta_-^{(1,2)}| = 2.7$ sec of arc which is just about large enough to make the separation possible. For higher harmonics it is even larger.

The experimental results as shown in Fig. 13 confirm that with proper alignment on the peak of the fundamental the suppression of higher harmonics is 3×10^{-3} for the first harmonic and that all other harmonics are close to 10^{-4} (Fig. 13 top). On the other hand, if alignment is made so that the 1st harmonic is maximized then both the fundamental and higher harmonics are present (Fig. 13 bottom), but lower energy "lines" can easily

be suppressed by suitable absorbers. We have also computed the theoretical rocking curves of the setting for λ = 1.54 Å and $\lambda/2$ for monochromatic radiation and zero-angular divergence and compared them qualitativly with measured curves (Fig. 14). Taking into account that the computed curves do not include any angular divergence, the agreement is quite satisfactory, especially with respect to the relative intensities for λ and $\lambda/2$ and also regarding the relative angular shift of the two rocking curves. The latter is the essential feature which makes the suppression of $\lambda/2$ against λ possible.

4.3 Combination of symmetrical Bragg and Laue case diffraction from equal crystals

In this case - $(\gamma_h/\gamma_o)_I = (\gamma_h/\gamma_o)_{II} = 1$. For the separation of the fundamental from the n-th harmonic we derive from (5)

$$\Delta\beta_-^{(1,n)} = \frac{r_e\lambda^2}{\pi}\left(1-n^{-2}\right)\frac{N}{\sin 2\Theta_B} \qquad (7)$$

For λ = 1.54 Å and the Si 220 reflection we calculate $|\Delta\beta_-^{(1,2)}|$ = 1.96 sec of arc. Again the higher harmonics have a larger separation from the fundamental. Obviously $\Delta\beta_-^{(1,n)}$ increases with n to the asymptotic value $\frac{r_e\lambda^2}{\pi}(N/\sin 2\Theta_B)$. Higher harmonics among themselves will thus barely be separable by

this method. A more exact treatment has to take into account the width of the single reflection curves and has to compare it with the angular shift $\Delta\beta_-^{(1,n)}$. A separation is impossible if $|\Delta\beta_-^{(1,n)}|$ is smaller than the average width of the reflection curves of the fundamental and harmonic. As may be seen from an exact calculation of Bragg case single crystal reflection curves (Fig. 15) carried out for the Si 220 reflection and λ = 1.54 Å there is a clear separation between the fundamental and higher harmonics.

The method just described was applied in the interferometric measurement (Bonse & Materlik, 1974) of anomalous dispersion near absorption edges. The setup used is shown in Fig. 16. The twofold symmetric Bragg reflection groove is used as fore crystal to the triple Laue case symmetric interferometer. Interference fringes are photographically recorded in the H and O beams. Alternatively, using the SSD-multichannel-analyser system, the wavelength spectrum is measured in either beam. Groove crystal and interferometer together represent a Bragg Laue case combination for the elimination of unwanted harmonics. The difference to the system discussed just before is that multiple reflections (twofold Bragg and threefold Laue) are used. Separation abilities are expected to improve even with multiple reflections.

Measurements of the spectrum are shown in Fig. 17 and corres-

ponding fringe patterns in Fig. 18.

In Fig. 17 the measured spectra of the O-beam (left) and the H-beam (right) are given. The spectra at the top are obtained when groove crystal and interferometer are aligned to maximum intensity of the fundamental. As is seen all harmonics are very weak. With the same alignment the interference fringe pattern (Fig. 18 left) has a spacing Λ which corresponds to the wavelength λ of the fundamental. Next the intensity of the first harmonic was maximized by small $\Delta\theta$-rotation of the interferometer with respect to the fore crystal (middle of Fig. 17). The first harmonic appears with an intensity about 12 times higher than the second harmonic and about 15 times higher than the fundamental. Correspondingly a fringe pattern with spacing 2Λ is observed with this alignment (Fig. 18, middle). In the bottom of Fig. 17 the spectrum is shown after the intensity of the second harmonic is maximized. Besides the second harmonic also the third one is seen to occur to some extent, which is to be expected from the imcomplete separation between the second and third harmonic reflection curves in Fig. 15. Nevertheless the corresponding fringe pattern has the expected spacing 3Λ (Fig. 18, right).

For interferometry, the successfull elimination of all harmonics is very important, since phase shifts are normally quite

different at $\lambda/2$, $\lambda/3$ etc. Especially for the measurement of the dispersion correction $\Delta f'$ near the absorption edge the elimination of all higher harmonics is essential. Detailed results of the $\Delta f'$ measurement of Ni near the K-edge will be published elsewhere.

We thank the European Molecular Biology Laboratory (EMBL) group for generous hospitality in their experimental site at DESY in Hamburg, and C. Kunz and E.E. Koch for technical advise and for providing the program used to calculate the intensity distributions of the DESY-X-radiation.

J. Barrington-Leigh, K.C. Holmes & G. Rosenbaum (1972): Proceedings of a Study Symposium held at Brookhaven Nat. Lab. Sept. 25-28

J.A. Beaumont & M. Hart (1974): J. of Physics E 7, 823-829

U. Bonse & M. Hart (1965): Appl. Phys. Lett. 7, 238

U. Bonse, G. Materlik & W. Schröder (1974): Conference on Synchrotron Radiation and its Application to the Analysis of Problems in Scientific Investigation, 1-2 April, Reading, GB

U. Bonse & G. Materlik (1974): Anomalous scattering, published for the Int. Union of Crystallography by Munksgaard, Int. Publishers, Copenhagen, Denmark , p. 107 - 109

U. Bonse & G. Materlik (1975): 10th Int. Congress of Crystallography, Amsterdam (to be published in Acta Cryst.)

J.W.M. DuMond (1937): Phys. Rev. 52, 872.

W. Ehrenberg & H. Mark (1927): Z. f. Physik 42, 807-822

M. Hart (1975): J. of Appl. Cryst. 8, No. 4, 436

K.C. Holmes (1974): Endeavour, Vol. XXXIII, No. 119

S. Kikuta & K. Kohra (1970): J. Phys. Soc. Jap. 29, 1322-1328

B.M. Kincaid & P. Eisenberger (1975): Phys. Rev. Lett. 34, 1361-1364

M. v.Laue (1960): Röntgenstrahlinterferenzen, Akad. Verlags-Ges., Frankfurt/M.

J. Schwinger (1949): Phys. Rev. 75, 1912-1925

T. Tuomi, K. Naukkarinen, E. Laurila & P. Rabe (1973): Acta Polytechn. Scand Ph 100, 1-4

T. Tuomi, K. Naukkarinen & P. Rabe (1974): Phys. Stat. Sol. (a) 25, 93-106

Fig. 1 Photons per sec at DESY under the experimental conditions given in the text; $\Delta\lambda = 10^{-3}$ Å, beam current 10 m A, curves 1, 2, 3, 4, 5 correspond to E_{max} = 4, 5, 6, 6.5, 7.2 GeV respectively.

Fig. 2 as Fig. 1 but curves 1, 3 for parallel and curves 2, 4 for perpendicular polarization and 5, 7.2 GeV respectively.

Fig. 3 as Fig. 1 but variation with the inclination angle Ψ against the orbit plane; 1, 3 for parallel and 2, 4 for perpendicular polarization and 1.5, 0.75 Å respectively; E_{max} = 5 GeV.

Fig. 4 as Fig. 3 but E_{max} = 7.2 GeV.

Fig. 5 Variation of photon numbers within the slit described in the text. Curves 1, 2, 3 for λ = 1.5, 0.75 and 0.32 Å respectively. Photons of states $\perp$ and $\parallel$ have been added. E_{max} = 5 GeV.

Fig. 6 as Fig. 5 but E_{max} = 7.2 GeV.

Fig. 7 Time dependence of photon rates within the accelerating cycle, see text. Curves 1, 2, 3, 4 for λ = 3, 1.5, 0.75, 0.32 Å respectively; E_{max} = 5 GeV.

Fig. 8 as Fig. 7, but E_{max} = 7.2 GeV.

Fig. 9 220-Si groove crystal monochromator. See Text.

Fig. 10 Spectrum behind the groove monochromator measured with a Si(Li)- SSD . Upper and lower curve with different Bragg angle. No corrections made for the energy dependence of the detection efficiency of the SSD. Note the presence of a large number of harmonics. E_{max} = 6 GeV.

Fig. 11 The double crystal diffractometer with (+, +) setting as a highly dispersive system, (a) beam paths; (b) DuMond diagram.

Fig. 12 The double crystal diffractometer with (+, -)-setting and $d_1 \neq d_2$ as a slightly dispersive system. (a) beam paths; (b) DuMond diagram.

Fig. 13 Spectrum of the slightly dispersive (+, -)-setting as shown in the insert.
top: The harmonics are suppressed by maximizing the fundamental.
bottom: For comparision the spectrum obtained when the first harmonic is maximized is shown.

Fig. 14 Comparison of computed and measured rocking curves see text, (+) ≈ Fundamental; (o) ≈ 1st harmonic.

Fig. 15 Calculated Bragg case single crystal reflection curves for the fundamental (220) and its first harmonics (440), (660). See text!

Fig. 16 Set-up used for the elimination of harmonics by combining a Bragg case groove with a Laue case interferometer.

Fig. 17 Spectra of the O-beam (left) and the H-beam (right) of the interferometer set-up of Fig. 16. See text.

Fig. 18 Fringe systems in the O-beam of Fig. 16 for the fundamental (left), 1st harmonic (middle) and 2nd harmonic (right).

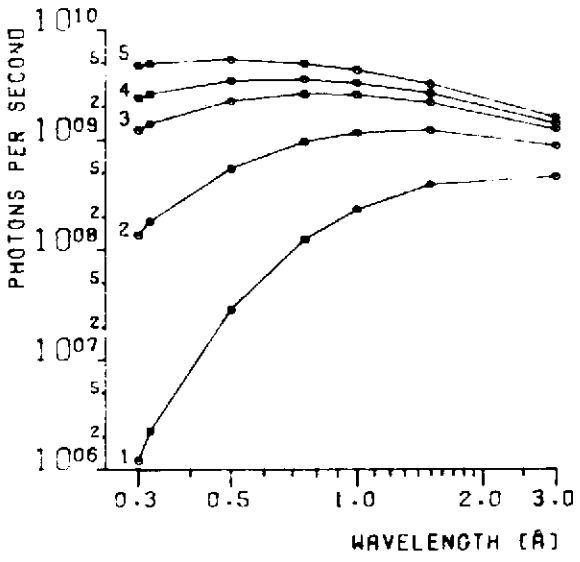

Fig. 1

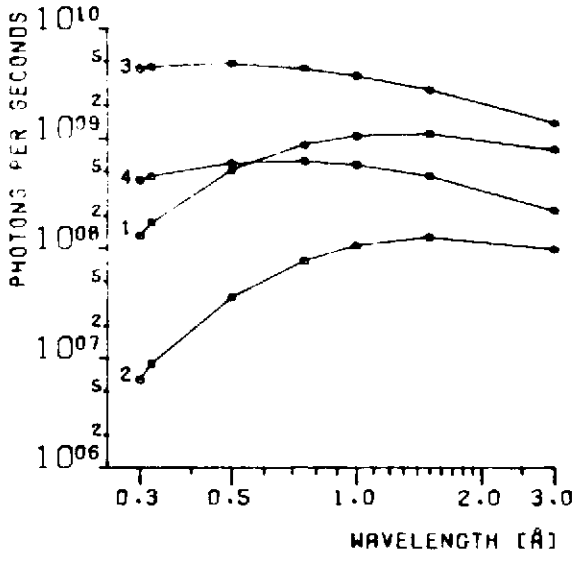

Fig. 2

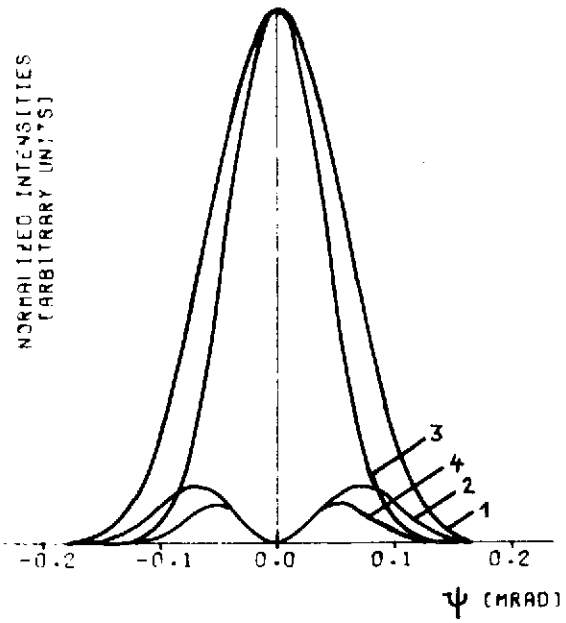

Fig. 3

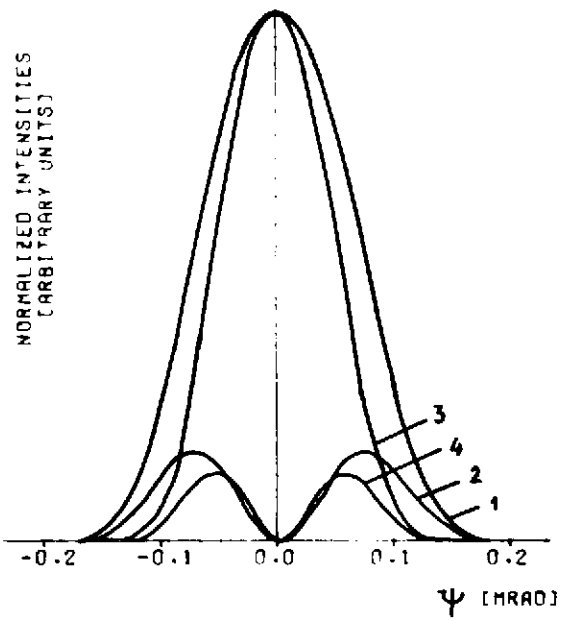

Fig. 4

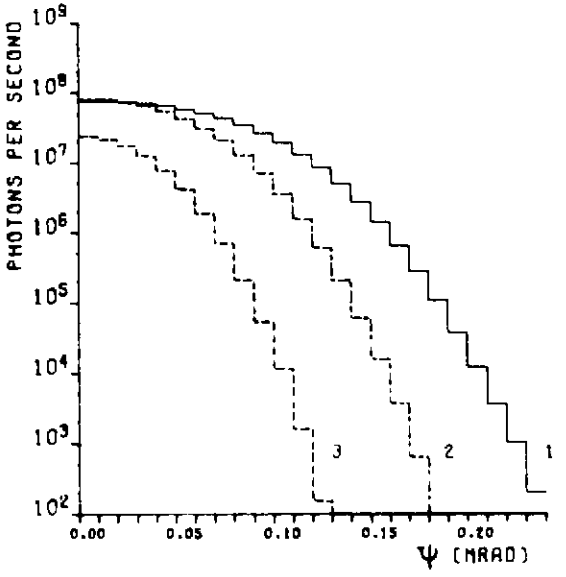
PHOTONS PER SECOND
10^9
10^8
10^7
10^6
10^5
10^4
10^3
10^2
0.00
0.05
0.10
0.15
0.20
Ψ [MRAD]
1
2
3

Fig. 5

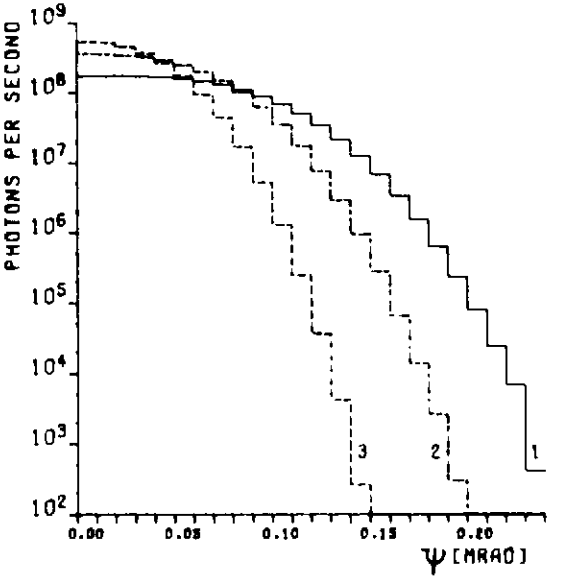
PHOTONS PER SECOND
10^9
10^8
10^7
10^6
10^5
10^4
10^3
10^2
0.00
0.05
0.10
0.15
0.20
Ψ [MRAD]
1
2
3

Fig. 6

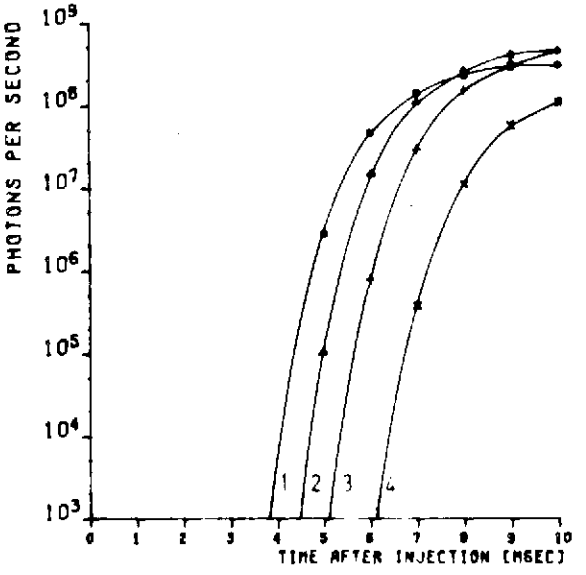
PHOTONS PER SECOND
10^9
10^8
10^7
10^6
10^5
10^4
10^3
1
2
3
4
0 1 2 3 4 5 6 7 8 9 10
TIME AFTER INJECTION (MSEC)

Fig. 7

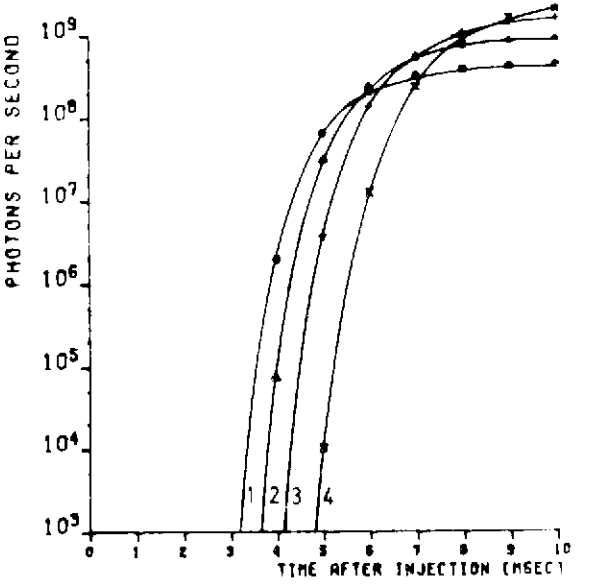
PHOTONS PER SECOND
10^9
10^8
10^7
10^6
10^5
10^4
10^3
1
2
3
4
0 1 2 3 4 5 6 7 8 9 10
TIME AFTER INJECTION (MSEC)

Fig. 8

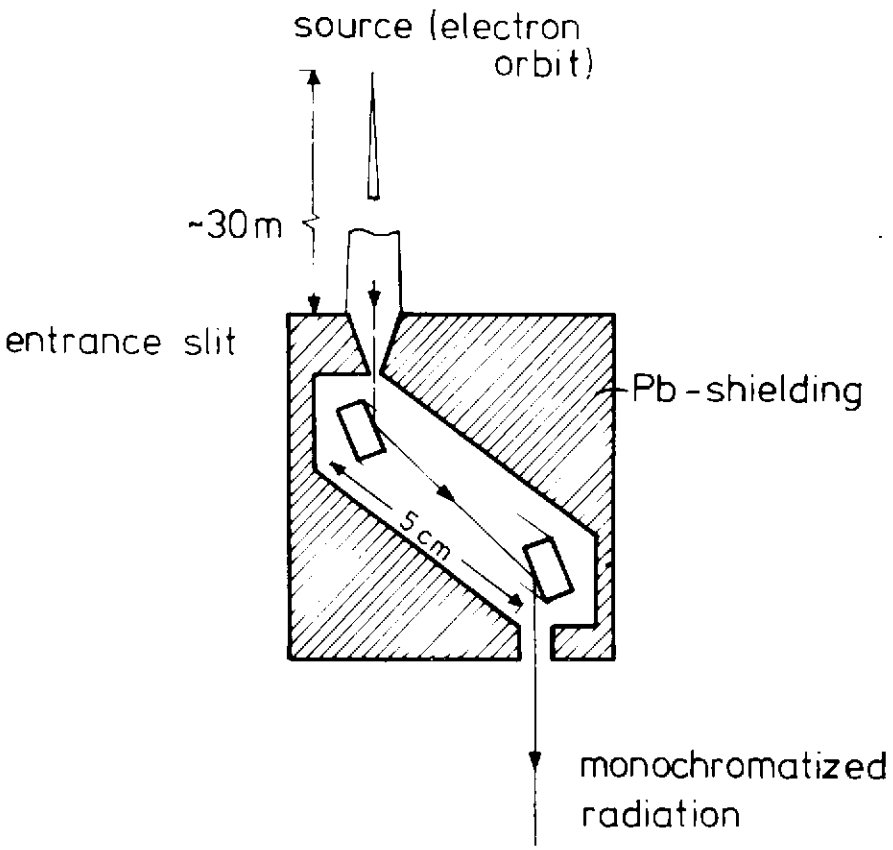
source (electron
orbit)
~30 m
entrance slit
Pb - shielding
5 cm
monochromatized
radiation

Fig. 9

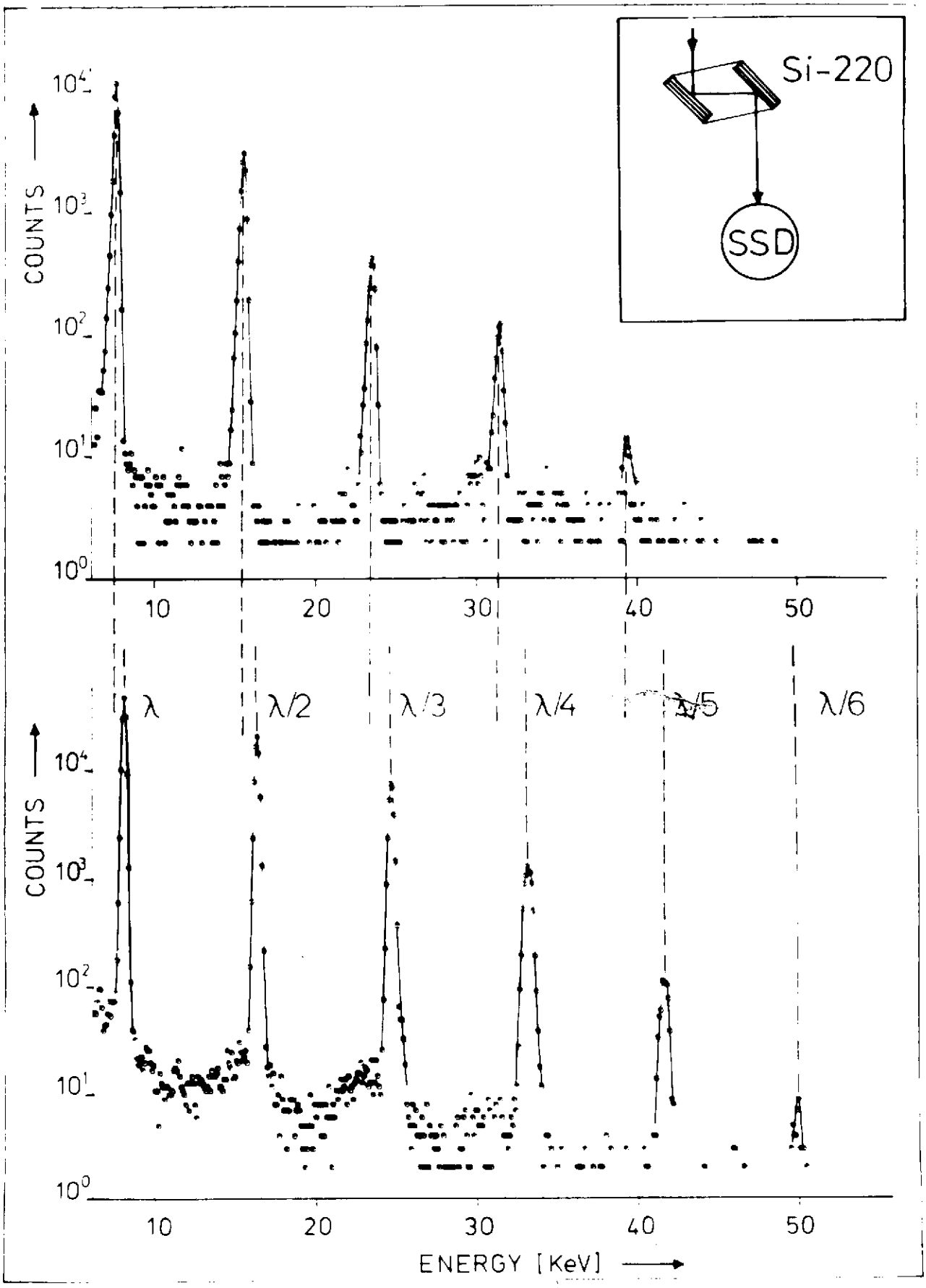
Si-220
SSD
COUNTS
10^4
10^3
10^2
10^1
10^0
10
20
30
40
50
λ
λ/2
λ/3
λ/4
λ/5
λ/6
ENERGY [KeV]

Fig. 10

Fig. 11a

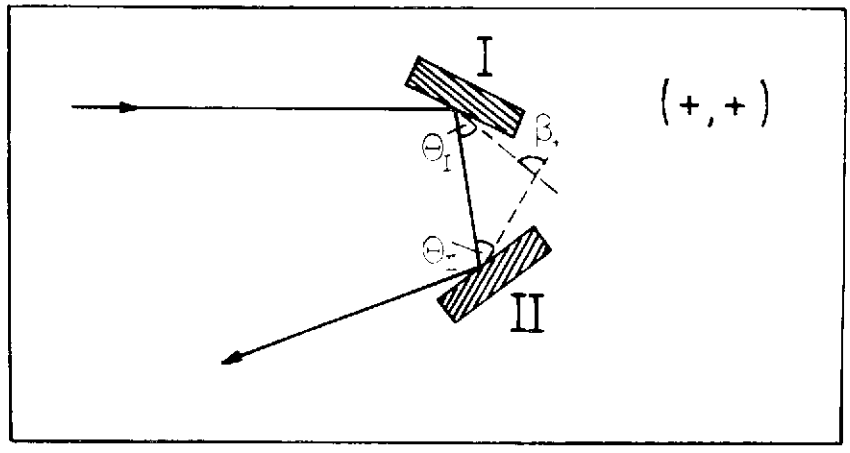

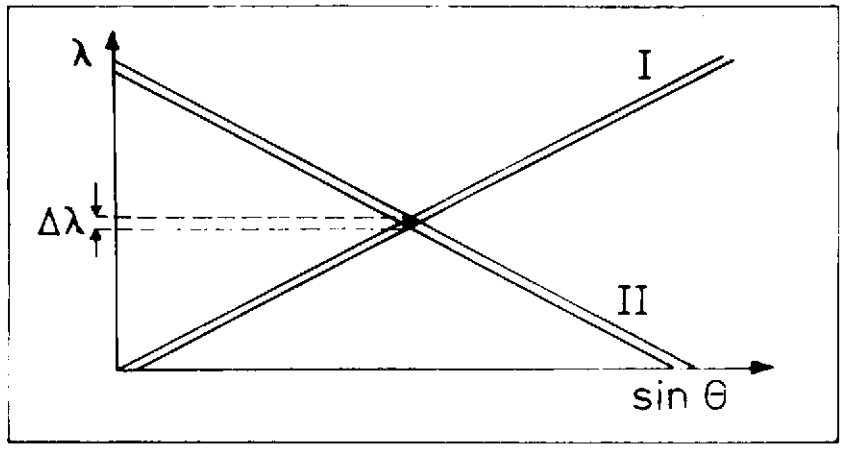

Fig. 11b

Fig. 12a

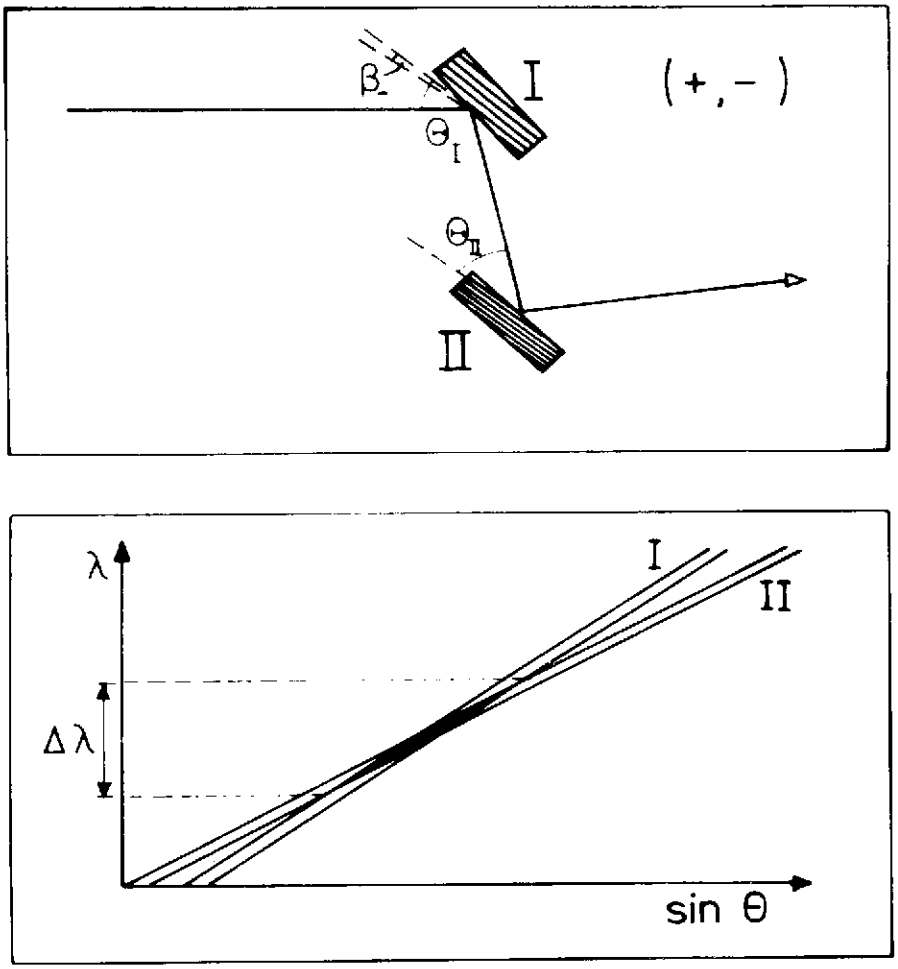

Fig. 12b

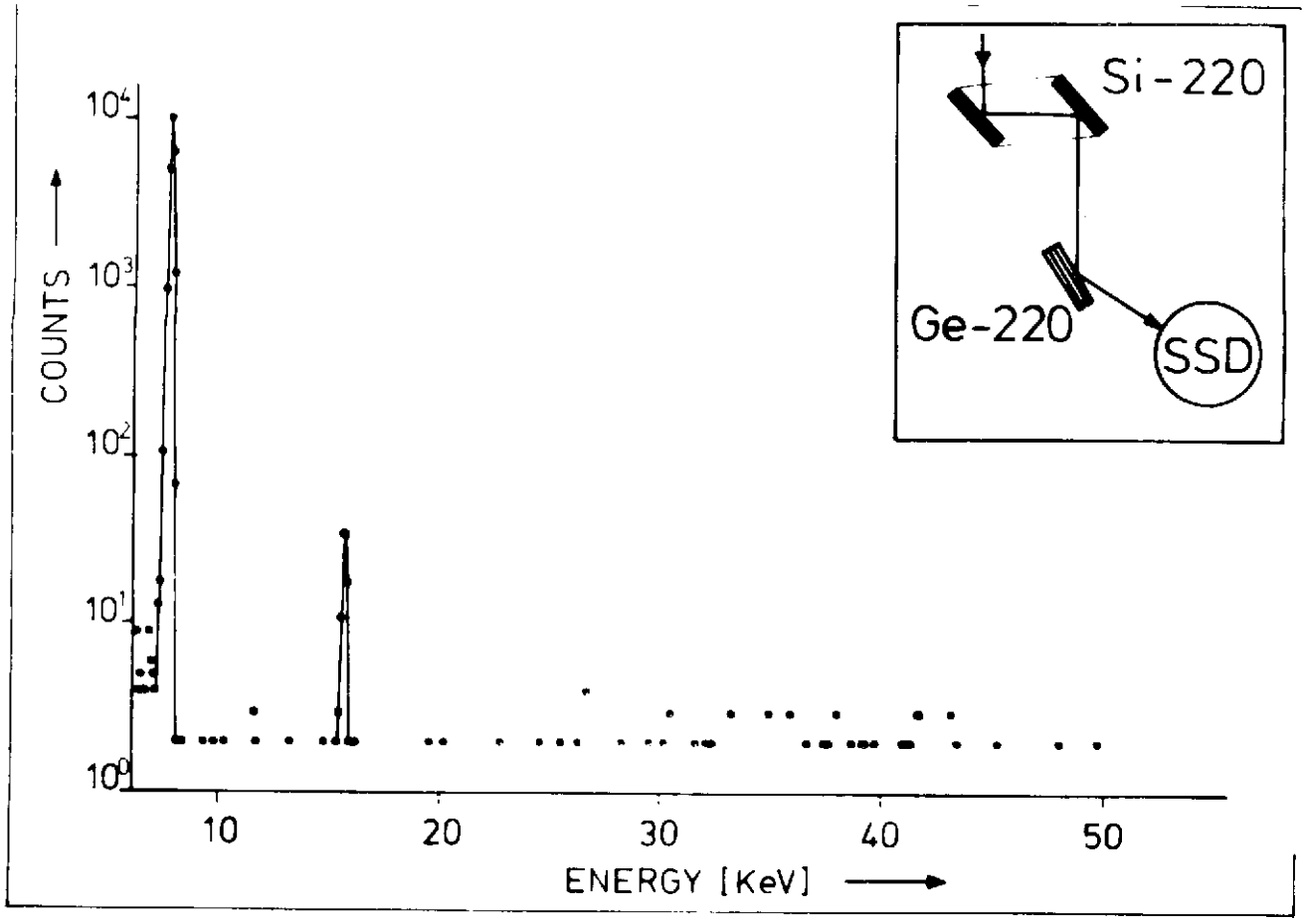
Si-220
Ge-220
SSD
COUNTS
10^4
10^3
10^2
10^1
10^0
10
20
30
40
50
ENERGY [KeV]

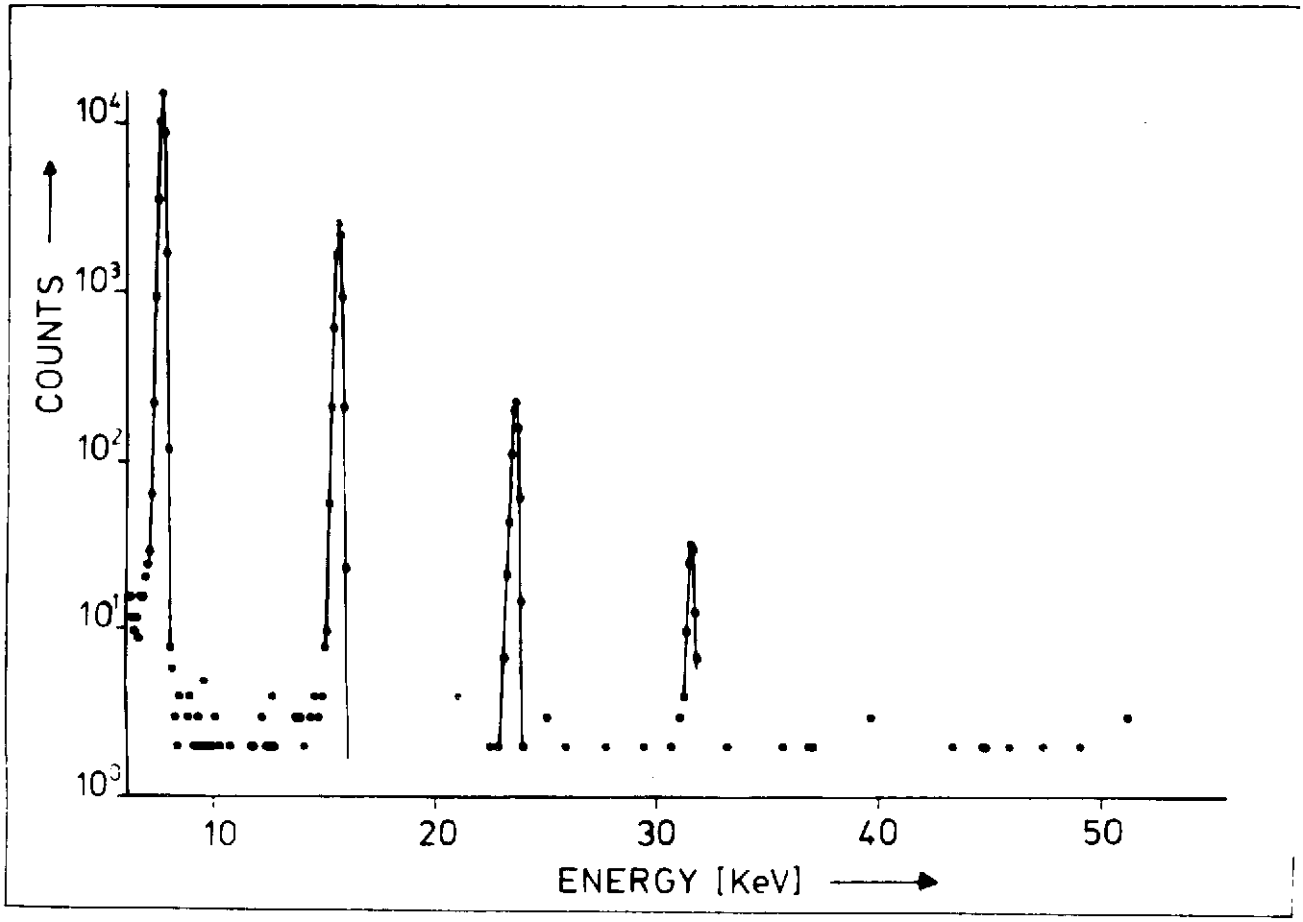
COUNTS
10^4
10^3
10^2
10^1
10^3
10
20
30
40
50
ENERGY [KeV]

Fig. 13

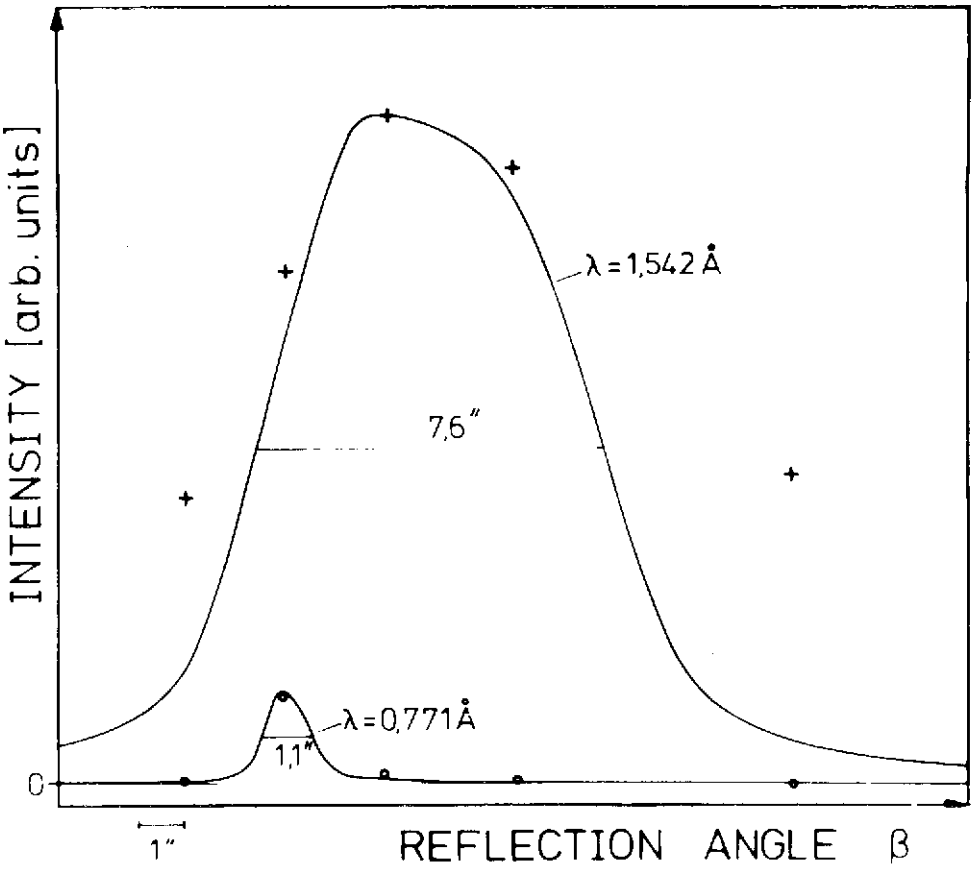
INTENSITY [arb. units]
λ = 1,542 Å
7,6"
λ = 0,771 Å
1,1"
0
1"
REFLECTION ANGLE β

Fig. 14

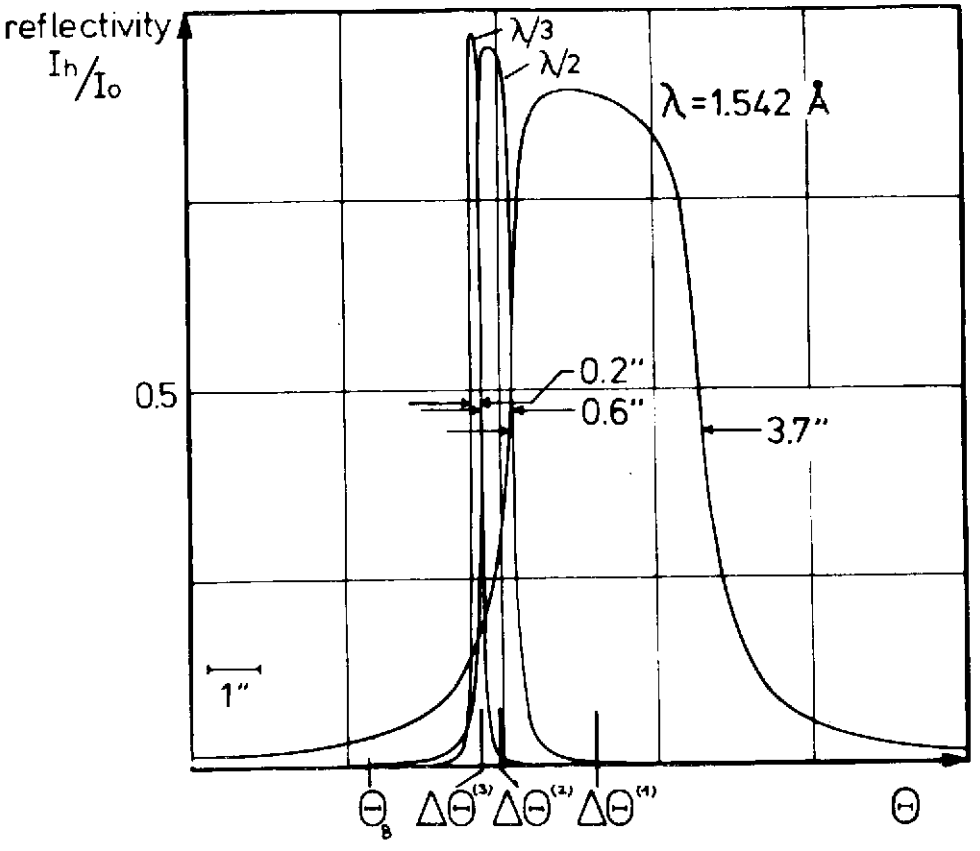
reflectivity
Ih/Io
λ/3
λ/2
λ=1.542 Å
0.2"
0.6"
3.7"
0.5
1"
ΘB
Δθ(3)
Δθ(2)
Δθ(1)
Θ

Fig. 15

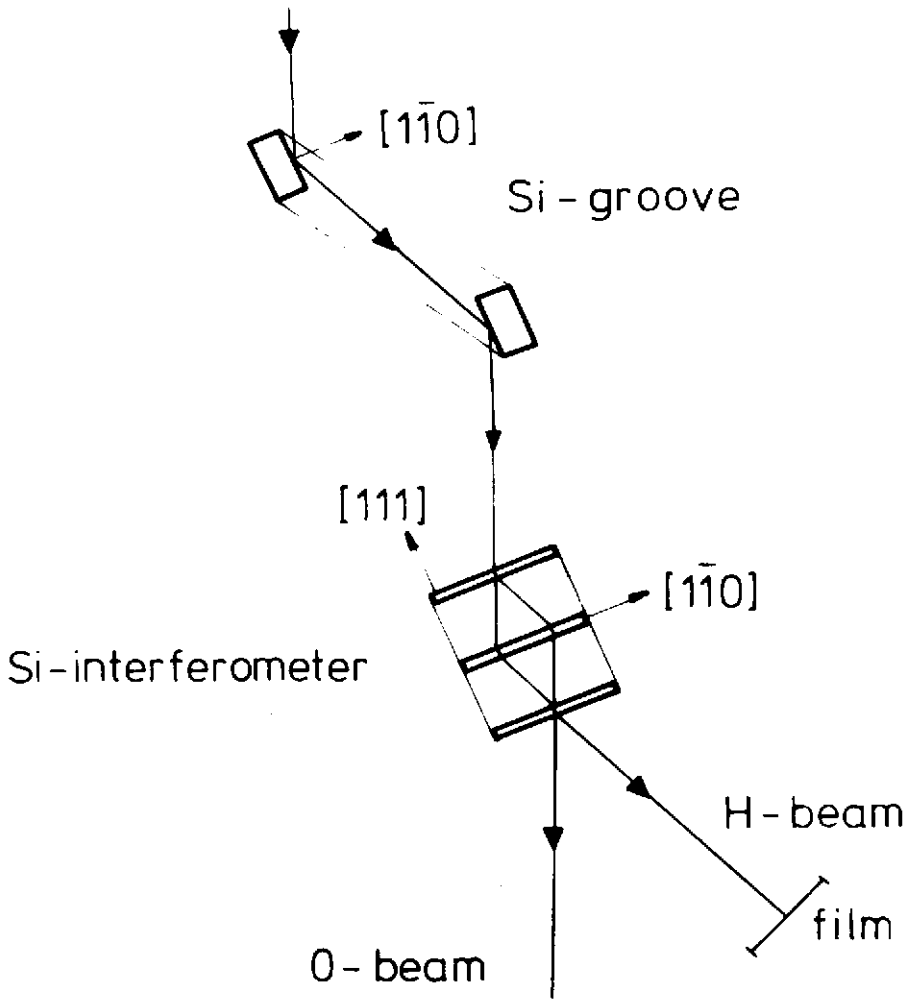
[1$\bar{1}$0]
Si - groove
[111]
[1$\bar{1}$0]
Si - interferometer
H - beam
film
0 - beam

Fig. 16

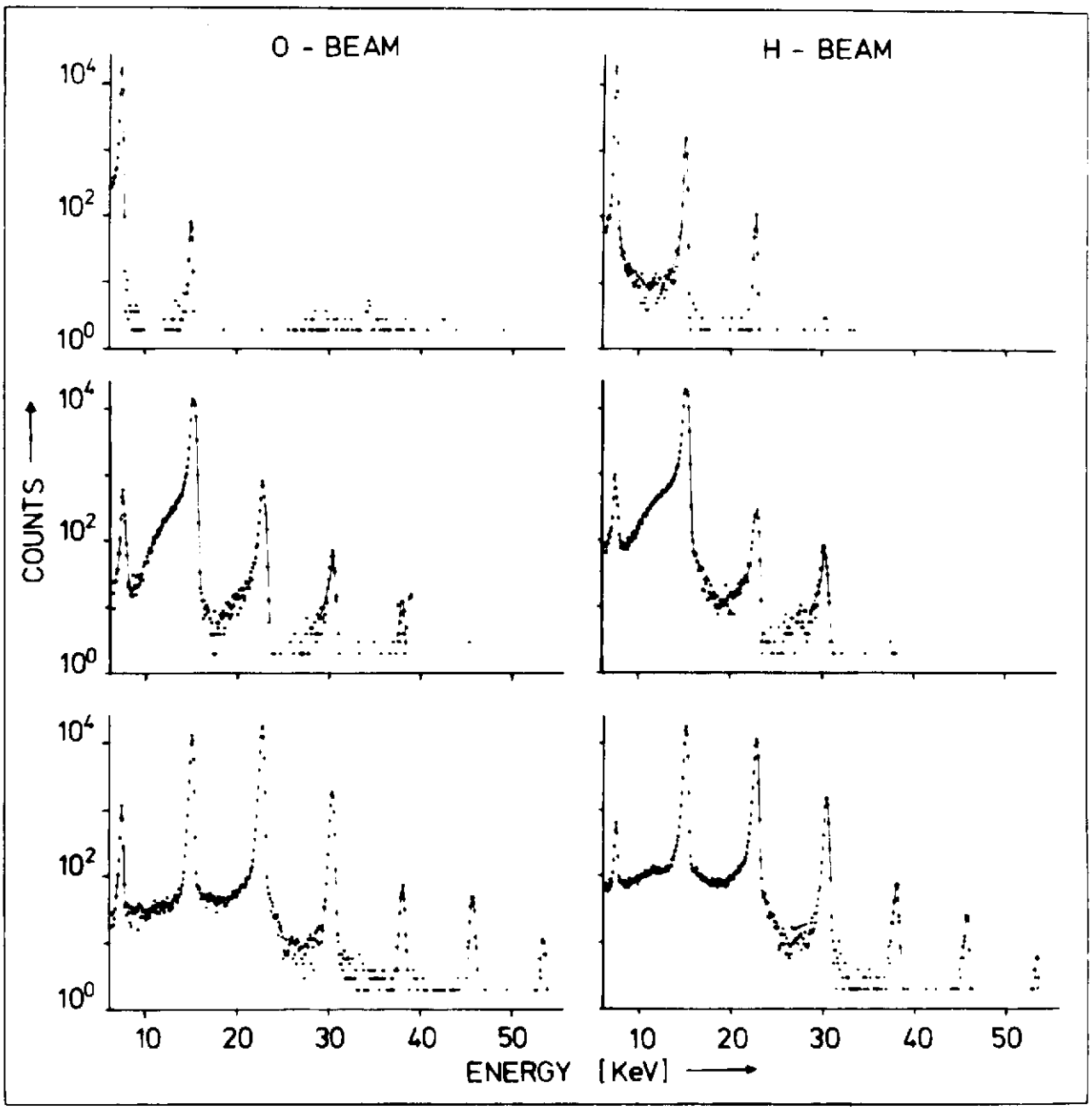

Fig. 17

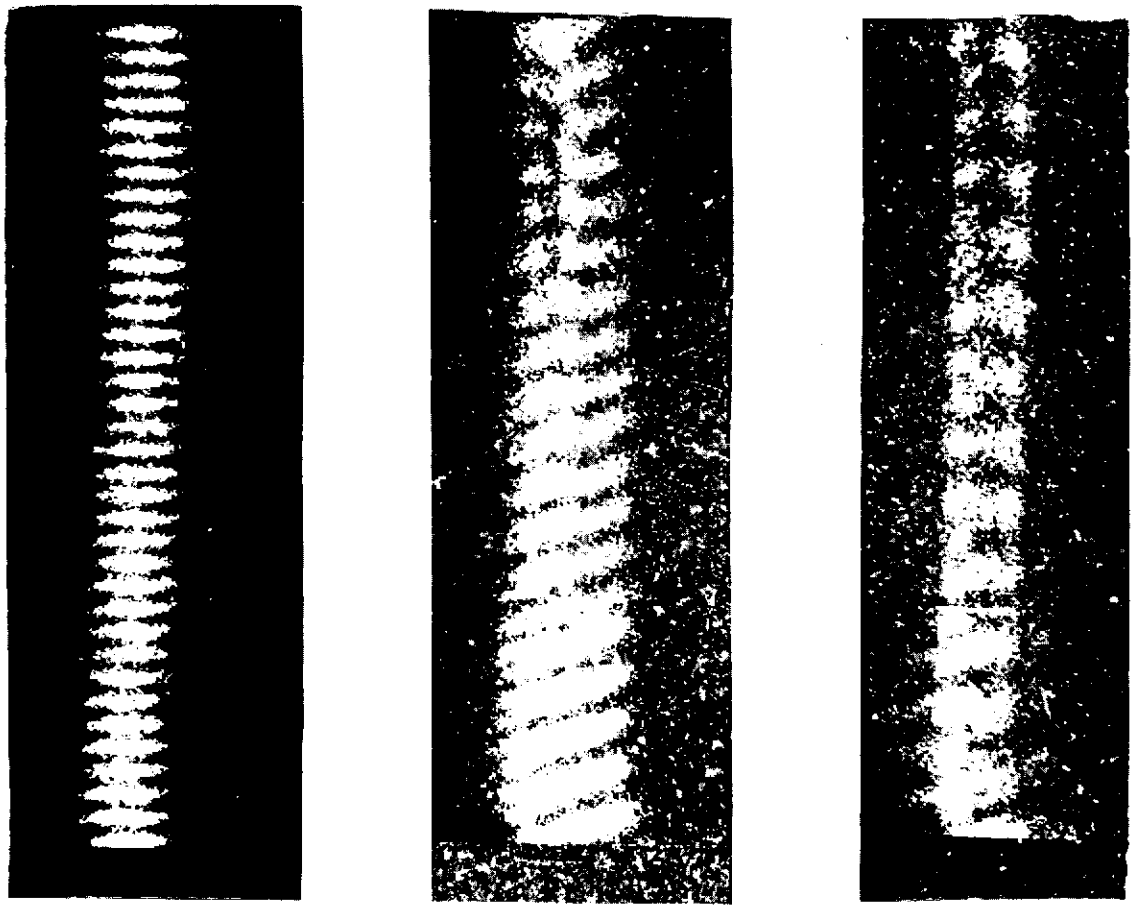

Fig. 18